

Energy-lowering symmetry breaking creates a flat-band insulator in paramagnetic Nb_3Cl_8

Jia-Xin Xiong,¹ Xiuwen Zhang,¹ and Alex Zunger^{1,*}

¹*Renewable and Sustainable Energy Institute, University of Colorado, Boulder, Colorado 80309, USA*

Ordinary band structure calculations of quantum materials often incorrectly predicted metallic, instead of insulating electronic structure, motivating Mott-Hubbard strong electron correlation as a gapping mechanism. More recently, allowing the formation of local structural symmetry breaking motifs in otherwise ordinary band theory was shown to lower the total energy while predicting insulating gaps when they are observed. An important counter example was recently pointed out whereby the flat band formed in Nb_3Cl_8 by symmetry breaking is by itself partially occupied, thus failing to account for the observed insulating state. It is shown here that a generalized symmetry breaking involving the cooperative structural and magnetic effects produces in mean-field-like density functional theory an energy lowering insulating phase.

Gap anomaly in Nb_3Cl_8 : A range of quantum materials manifest local microscopic degrees of freedom nested within the average crystallographic structure. Such local motifs are experimentally observable by local structural probes [1,2] and calculable quantum mechanically as energy-lowering symmetry breaking motifs [3,4]. Symmetry breaking can split off narrow flat bands [5–8] from a broad conduction band (as in LaTiO_3 and VO_2), or from the broad valence band (as in LaFeO_3 and SrBiO_3), leading in a single step to the observed insulating phases in these quantum oxides. This offers a link between energy gap formation and the local structural motifs traditional in solid-state chemistry, such as Peierls instabilities, Jahn-Teller distortions, or bond disproportionation, both in d-electron (such as LaMnO_3 [9] and NbO_2 [10]) or in non-d-electron compounds (such as BaBiO_3 [11]). It was recently pointed out [12,13] that α -phase Nb_3Cl_8 is special among other quantum materials in that symmetry breaking (here, Nb-Nb-Nb trimer formation) creates a partially occupied band in the ground state, hence the system remains metallic whereas the observed α -phase [12,13] is insulating. This discrepancy opens the possibility that α -phase Nb_3Cl_8 (see Supplemental Section A on the structures) is the long-sought example where purely electronic strong correlation, encoded by the Mott-Hubbard approach [14] in a fixed crystallographic structure, is not just a textbook illustration, but is required for explaining gapping unobtainable by uncorrelated physics.

The significance of this discovery: This triumph [12] is far from being trivial. It requires avoidance of numerous alternatives explainable via conventional band structure such as density functional theory (DFT). Had the composition of the measured sample been Cl-richer (such as Nb_3Cl_9) or one where one Cl atom would be replaced by Te (such as in $\text{Nb}_3\text{Cl}_7\text{Te}$ [15]), the correct insulating phases would be guaranteed by the trivial closed-shell configuration. Structural and magnetic symmetry breaking must be examined, although they were rejected to establish a compelling alternative scenario for insulation via strong correlation. For example, the sister d-electron compound NbO_2 is predicted by DFT to be a metal with-

out any structural symmetry breaking, but once Peierls-like symmetry breaking of Nb-Nb dimerization is examined [16], it shows total energy stabilization, concomitantly with becoming an insulator, in agreement with experiments without need for strong correlation Hubbard description [Figure 1(a, b)]. Also, other perovskites like SrVO_3 [17] and LaNiO_3 [18] are predicted by DFT to be metals, and structural or magnetic symmetry breaking is too weak to convert them to insulators. However, the predicted metallic states in the former oxides are the correct experimental reality for these two compounds [19–21], unlike the case for the insulating α -phase of Nb_3Cl_8 .

The question posed: Can symmetry breaking—either structural or magnetic, or both—lower the total energy, while also opening a band gap? Here we examine the possible role of magnetism in explaining the insulation of Nb_3Cl_8 . We use the DFT exchange-correlation functional [22] meta-generalized gradient approximation (meta-GGA) to calculate the electronic structures without Coulomb repulsion U . The DFT method details are provided in Supplemental Section B.

Structural symmetry breaking in nonmagnetic NbO_2 suffices to correctly describe it as an insulator: Before considering Nb_3Cl_8 , we first glance again at its simpler sister compound NbO_2 . This compound has a metal-insulator transition with two nonmagnetic phases whose crystal structures are both tetragonal but different in formation of Nb-Nb dimers. As shown in Fig. 1(a, b), the high-temperature (high- T) phase has the Fermi level residing in the broad principal conduction band and is metallic because it has no Nb-Nb dimers [Fig. 1(a)]. As shown in Fig. 1(c, d) the low-temperature (low- T) phase has Nb-Nb dimerization [Fig. 1(c)]. This dimerization constitutes structural symmetry breaking which stabilizes the total energy by 152 meV/formula unit relative to the metallic phase and splits off occupied flat bands from the principal conduction band down into the internal energy gap, thereby opening a band gap [Fig. 1(b)]. The states of the split-off flat bands in the low- T insulating phase are mainly localized on the Nb-Nb dimers [Fig. 1(d)], while the states near the Fermi level in the high- T metallic phase surround the Nb atoms [Fig.

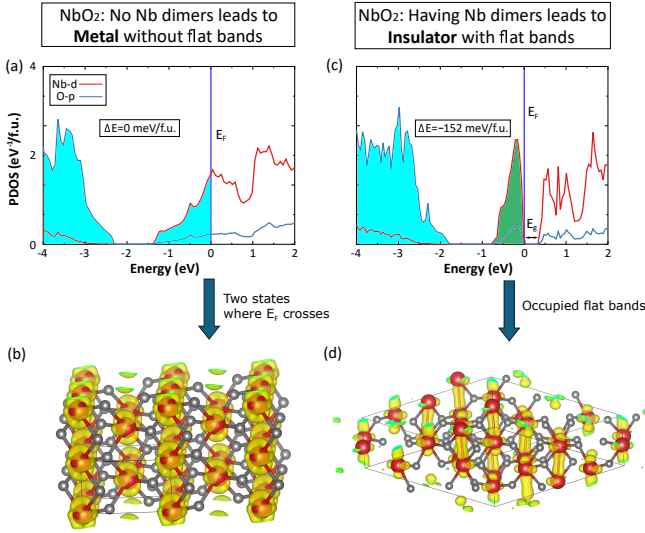


FIG. 1: Two phases of nonmagnetic tetragonal NbO_2 . (a, b) The metallic phase without Nb dimers and (c, d) the insulating phase with Nb dimers creating occupied flat bands. (a, c) The partial densities of states (PDOS) decomposed into Nb-d (red) and O-p (blue) orbitals. The filled blue and green colors in (a, c) represent the occupied states. The filled green color in (c) emphasizes the occupied split-off flat bands in the insulating phase. (b, d) The partial charge density distributions for the states (b) near the Fermi level and (d) occupied flat bands. The partial charge densities use the isosurface of 0.035 and 0.025 e^-/bohr^3 , respectively. The dark red and grey balls represent Nb and O atoms, respectively.

1(b)].

The structural symmetry breaking in Nb_3Cl_8 retains the incorrect metallic phase: The compound Nb_3Cl_8 is more complex than its sister compound NbO_2 in terms of the structural symmetry breaking, paramagnetism and thus band gap opening mechanism. Nb_3Cl_8 is a layered material where each layer has Nb trimers forming the distorted Kagome lattice with a breathing mode [12,23]. Each Nb trimer is surrounded by 13 Cl ions, forming an $\text{Nb}_3\text{Cl}_{13}$ cluster $[\text{Nb}_3\text{Cl}_8]^{5+}[\text{Cl}_5]^{5-}$. Here a Nb trimer has 15 electrons but 8 of them are transferred to Cl_8 , so 7 electrons are left per cluster. They occupy the molecular orbitals configuration $(1a_1)^2(1e)^4(2a_1)^1$ so that the highest occupied molecular orbital (HOMO) is singly occupied for the nonmagnetic Nb trimer cluster. By comparing the band structures of monolayer and bilayer structures for the α -phase Nb_3Cl_8 , Supplemental Section C shows that the interlayer coupling does not influence the metallic state of the non-magnetic phase. Thus, subsequent calculations are performed by using the monolayer structure. The Nb-Nb-Nb trimerization in α -phase Nb_3Cl_8 is observed experimentally, showing short intra-cluster Nb-Nb bond length $d^{\text{short}}(\text{Nb}-\text{Nb})$ of 2.834 Å and long intercluster Nb-Nb bond length $d^{\text{long}}(\text{Nb}-\text{Nb})$ of 3.998 Å [24]. The DFT structural relaxed calculations giving intracluster distance of 2.85 Å and intercluster of 4.02 Å are close to the experimental measurement [24].

We define the “degree of trimerization” (DOT) as:

$$\text{DOT} = \frac{d^{\text{long}}(\text{Nb}-\text{Nb}) - d^{\text{short}}(\text{Nb}-\text{Nb})}{d^{\text{long}}(\text{Nb}-\text{Nb}) + d^{\text{short}}(\text{Nb}-\text{Nb})} \times 100\%. \quad (1)$$

The DOT for the DFT relaxed structure and for the experimental structure [24] are both estimated to be 17.0%. The calculated total energy gives an enormous stabilization of 3365 meV/f.u. but the system is a band structure metal.

Paramagnetism in α -phase Nb_3Cl_8 : The paramagnetic (PM) α -phase of Nb_3Cl_8 was observed experimentally by measuring the magnetic susceptibility as a function of temperature, which was well fitted to the Curie-Weiss function giving rise to an effective PM Bohr magneton of $1.65 \mu_B$ [12]. This paramagnetism is not considered relevant to gapping in the strongly correlated approach. In such Mott model, magnetic exchange J deciding magnetism is modeled perturbatively in terms of Mott-ness strong Coulomb repulsion $J \sim 1/U$, leading to the expected weak or no magnetism when a large Coulomb U is selected. Here, we do not exclude the PM configuration.

Description of paramagnetic symmetry breaking: We compute PM non-perturbatively using magnetic exchange interactions J obtained from spin polarized DFT. The PM configuration is not replaced a priori by the nonmagnetic structure where each site has zero moment. The latter view assumes that the local symmetry equals the average crystal structure of global symmetry. Instead, a PM configuration can be described more generally as a distribution of non-zero local magnetic moment. We use for this purpose a “specially constructed” [25] supercell consisting of n Nb_3Cl_8 formula units (where n is a size convergence parameter and we use $n=16$ here) with zero global magnetization. Much like “special k -points for Brillouin zone integrating” [26,27], the spin-special quasirandom structure (spin-SQS) method is not a single snapshot but represents a configurational average. Indeed, the spin-SQS searches for a magnetic configuration that best matches the target multisite spin-spin correlation function with the given short-range order. The local magnetic moments are decided by DFT energy minimization and charge self-consistency starting from the optimal spin-SQS magnetic structure. Since the band structure of PM phase in a small Brillouin zone (corresponding to a real space supercell) is inconveniently dense to observe important information such as band dispersion, we unfold the band structure into the original Brillouin zone thereby obtaining effective spectral functions [28] that have, unlike conventional band structure, natural energy-dependent intensities and “fuzziness”.

The important observation regarding magnetic symmetry breaking: Once structural symmetry breaking (Nb trimerization) is accounted for, we find that magnetic symmetry breaking opens a gap in the PM phase, explaining the insulating phase without recourse to strong correlation or to dynamic effects. This is described next by breaking the process into steps that clarify the indi-

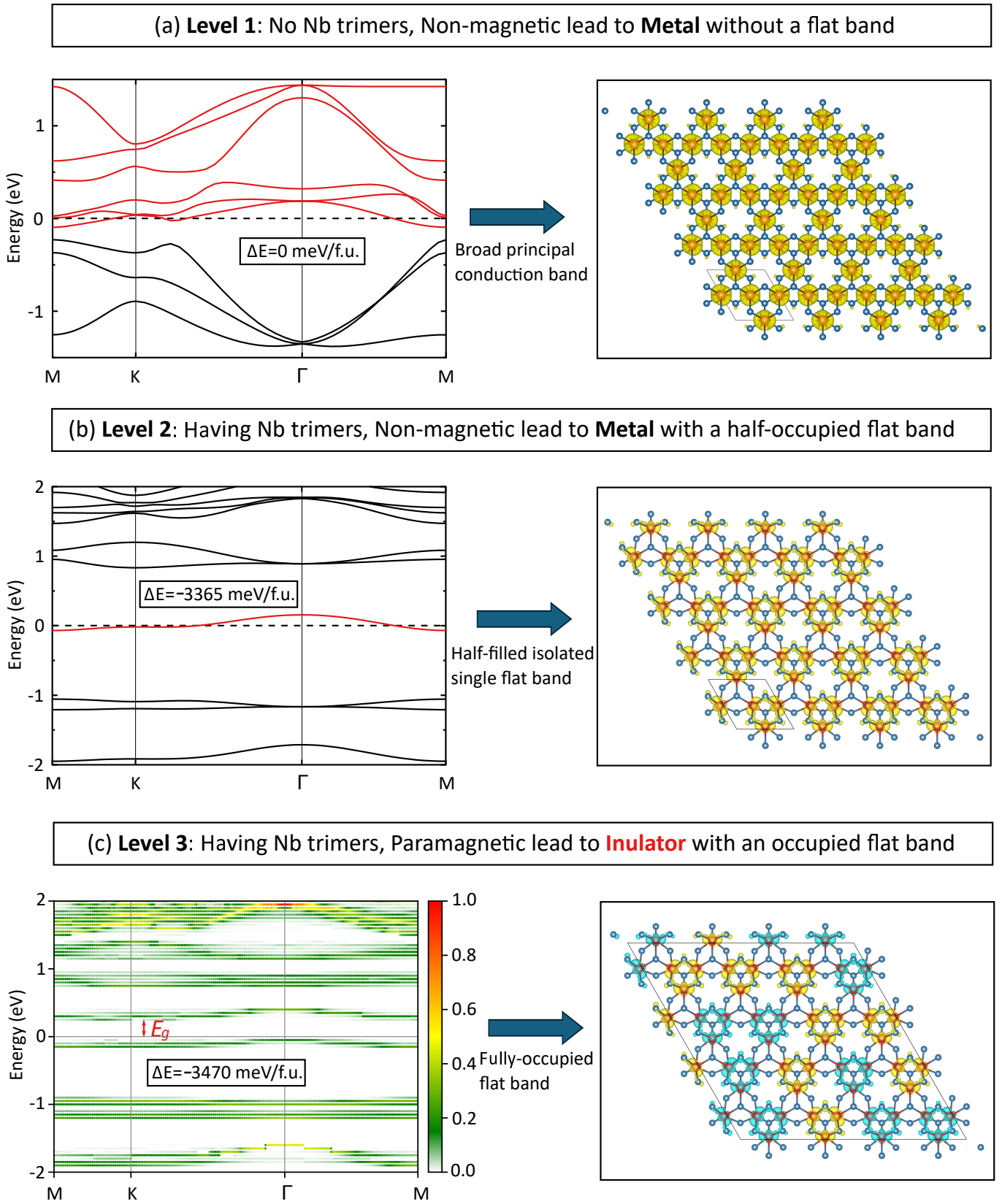


FIG. 2: Three levels of monolayer Nb_3Cl_8 including the band structures (left panels) and (magnetic) partial charge densities near the Fermi level (right panels). (a) Level 1: Non-magnetic phase (1 f.u. unit cell) having no Nb trimers leads to metal without a flat band. (b) Level 2: Non-magnetic phase (1 f.u. unit cell) having Nb trimers leads to metal with an isolated half-filled flat band marked in red in the band structure. (c) Level 3: Paramagnetic phase having Nb trimers leads to insulator. The unfolded band structure is obtained by projecting the states of 16 f.u. supercell onto primitive cell with the color bar representing the spectral function. The yellow and shallow blue color in magnetic charge density mean positive and negative magnetic densities, respectively. The partial charge densities in (a, b) use the isosurface of 0.02 and 0.008 $|e|/\text{bohr}^3$, respectively, and the magnetic density in (c) uses the isosurface of 0.004 $|e|/\text{bohr}^3$. The red and blue balls represent Nb and Cl atoms, respectively.

vidual contributions.

Hierarchy of symmetry breaking: Figure 2 demonstrates the three successive levels of theoretical description of monolayer Nb_3Cl_8 based on the existence or absence of two symmetry breaking modes—Nb trimerization and magnetic symmetry breaking.

Level 1 (symmetry unbroken) is for the hypothetical structure without Nb trimerization and magnetism. As shown in Fig. 2(a), the Fermi level lies within a broad principal conduction band with its charge density distributed equally on the Nb atoms. This configuration is taken as the total energy reference $\Delta E=0$.

In *Level 2* (structural symmetry breaking) with the Nb trimerization, we find that the Nb trimerization stabilizes the total energy by 3365 meV/f.u. relative to Level 1 and induces a single half-occupied isolated flat band at the Fermi level. This isolated flat band with band width of ~ 0.3 eV emerges from the broad principal conduction band of Level 1 and its charge density is dominantly located around the Nb trimers, as shown in Fig. 2(b). For the bilayer structure of nonmagnetic α -phase Nb_3Cl_8 , there are two split-off flat bands crossing with the Fermi level that are degenerate at H point (See Supplemental Section B). Evidently, in both monolayer and bilayer structures of α -phase Nb_3Cl_8 , the Nb trimerization with the formation of partially occupied split-off flat bands cannot open a band gap.

In *Level 3* (structural and magnetic symmetry breaking) that considers both (i) Nb trimers due to structural symmetry breaking and (ii) magnetic symmetry breaking. The latter is depicted as PM spin-SQS with self-consistently determined distribution of local moments, as shown in Fig. 2(c). This shows that the half-filled isolated flat band of Level 2 split forming two isolated flat bands and creating a band gap of 0.3 eV. It increases to 1.2 eV when using the HSE06 exchange correlation functional instead of SCAN. This process from Level 2 to Level 3 reduces the total energy by 105 meV/f.u. The band gap is opened by interaction of (i) structural symmetry breaking (forming trimers) and (ii) magnetic symmetry breaking. We find that the band gap cannot be opened if there is only one of the two symmetry breaking modes. This shows that one can predict the insulating phase of such quantum materials without Hubbard U .

Distribution of local motifs: To further indicate the difference between PM and nonmagnetic phases, Figure 3 shows the distribution of local magnetic moments in PM Nb_3Cl_8 (Level 3). It is observed that: (i) All of these results present a distribution of non-zero local magnetic moments and an average zero net magnetic moment, which is independent of the exchange correlation functionals and supercell sizes; (ii) The distribution of magnetic moments for SCAN and HSE06 is very different partially due to the strong exchange interaction in HSE06, but the choice of different exchange correlation functionals do not qualitatively change our main point that PM is essential to open the band gap.

Discussion: The PM phase lacks the long-range order

of the AFM phase but has short-range order that can still be essential to open the band gap. Indeed long-range antiferromagnetic order is well known [29] to enable insulating gaps. However, the absence of long-range magnetic order as the case in PM phase can, in the presence of short-range order lead either (i) to metallic phase if symmetry breaking is weak, as in SrVO_3 [3,17] and LaNiO_3 [30,31], or (ii) to an insulating PM phase, as in MnO , FeO , CoO , and NiO . Furthermore, symmetry breaking can induce other effects such as effective mass enhancement [17] without strong correlation.

The present results indicate that approximating the PM as nonmagnetic configuration and using primitive unit cell as input to do the calculations is not appropriate, missing energy lowering and gapping. Compared to nonmagnetic NbO_2 that only needs structural symmetry breaking (Nb-Nb dimerization) to open a band gap (Fig. 1), α -phase Nb_3Cl_8 is more complicated because it needs both structural (Nb-Nb-Nb trimerization) and magnetic (PM) symmetry breaking modes (Fig. 2).

The insulating bilayer nonmagnetic β -phase Nb_3Cl_8 : Besides the high- T PM α -phase, Nb_3Cl_8 has a low- T nonmagnetic β -phase, which is measured also as an insulator [12]. Because of the proximity of the layers in the β -phase, we allow in this case interlayer interaction via adding the Van der Waals (VdW) dispersive forces to the regular DFT. These dispersive forces have no influence on the α -phase but shorten the interlayer distance and increase the coupling within the bilayer β -phase. We find that in nonmagnetic β -phase Nb_3Cl_8 with two chemical formulae in the primitive cell, there are two split-off flat bands crossing with the Fermi level that are not degenerate at any k -points (see Supplemental Section C). This energy splitting is induced by the interlayer interaction. Therefore, in the β -phase the Nb trimerization and coupling of Nb trimers from adjacent layers have the potential to open a band gap, even without magnetism or strong correlation. Supplemental Section C provides a few tests of the insulating gap under different crystal structural parameters. A detailed study of the insulating gap in β -phase Nb_3Cl_8 is however beyond our scope as the details of the interlayer geometry are unknown.

Many-body physics is certainly to be preferred over single particle theory for understanding multiplet effects in electronically isolated ions in the gas phase [32,33], or for d -electron ions in wide-gap solids [34,35], etc. Many-body effects certainly exist as spectroscopic multiplet effects [36,37] and in multi excitons. Still, multi-electron effects that are often apparent in isolated ions such as carbon [38] often “melt away” when such atoms bond in condensed phases—as is the case when diamond or graphite are formed from carbon atoms. So, the question is: when is a many-electron treatment unescapable? But we see that the outlier phenomenology of gapping, the unusual case of Nb_3Cl_8 is describable by conventional DFT while reproducing also observable structural (Nb-Nb-Nb trimerization) and magnetic (the stabilization of a PM) symmetry breaking. This leads to an interesting

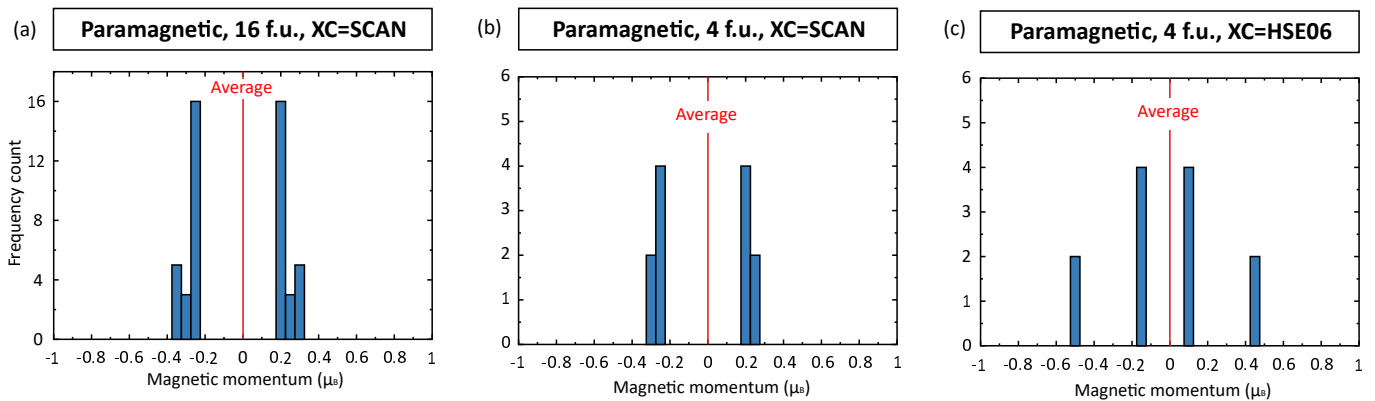


FIG. 3: Distribution of local magnetic moments in paramagnetic monolayer Nb_3Cl_8 simulated by different sizes of supercells using different exchange correlation (XC) functionals: (a) 16 formula-unit supercell by SCAN functional, (b) 4 formula-unit supercell by SCAN functional, and (c) 4 formula-unit supercell by HSE06 functional. The red solid lines at zero magnetic moment represent the average magnetic moment to be zero. The bin width of magnetic moment for plot is $0.05 \mu_B$.

duality: How will the band gap change if both the observable symmetry breaking (discussed in the present work) and the strong correlation Mott-Hubbard treatment used successfully in Ref. [12,23] to obtain gapping (without magnetic symmetry breaking) have important influences in producing an insulating phase? This remained question will inspire future research.

Acknowledgments

We thank Dr. Shunye Gao for discussions of his paper denoted here as Ref. [12]. This work was supported by the U.S. Department of Energy, Office of Science, Basic Energy Sciences, Materials Sciences and Engineering Division under Grant No. DE-SC0010467. This work used resources from the National Energy Research Scientific Computing Center (NERSC), which was supported by the Office of Science of the U.S. Department of Energy.

Reference

[1] A. N. Beecher, O. E. Semonin, J. M. Skelton, J. M. Frost, M. W. Terban, H. Zhai, A. Alatas, J. S. Owen, A. Walsh, and S. J. L. Billinge, Direct observation of dynamic symmetry breaking above room temperature in methylammonium lead iodide perovskite, *ACS Energy Lett.* 1, 880 (2016).
 [2] E. S. Božin, C. D. Malliakas, P. Souvatzis, T. Profen, N. A. Spaldin, M. G. Kanatzidis, and S. J. L. Billinge, Entropically stabilized local dipole formation in lead chalcogenides, *Science* 330, 1660 (2010).
 [3] O. I. Malyi and A. Zunger, False metals, real insulators, and degenerate gapped metals, *Appl. Phys. Rev.* 7, 041310 (2020).
 [4] X.-G. Zhao, Z. Wang, O. I. Malyi, and A. Zunger, Effect of static local distortions vs. dynamic motions on

the stability and band gaps of cubic oxide and halide perovskites, *Materials Today* 49, 107 (2021).

[5] Z. Zhu, H. Peelaers, and C. G. Van De Walle, Electronic and protonic conduction in LaFeO_3 , *J. Mater. Chem. A* 5, 15367 (2017).
 [6] M. Eaton, A. Catellani, and A. Calzolari, VO_2 as a natural optical metamaterial, *Opt. Express* 26, 5342 (2018).
 [7] F. El-Mellouhi, E. N. Brothers, M. J. Lucero, I. W. Bulik, and G. E. Scuseria, Structural phase transitions of the metal oxide perovskites SrTiO_3 , LaAlO_3 , and LaTiO_3 studied with a screened hybrid functional, *Phys. Rev. B* 87, 035107 (2013).
 [8] J. Varignon, J. Santamaria, and M. Bibes, Electrically switchable and tunable Rashba-type spin splitting in covalent perovskite oxides, *Phys. Rev. Lett.* 122, 116401 (2019).
 [9] H. Sawada, Y. Morikawa, K. Terakura, and N. Hamada, Jahn-Teller distortion and magnetic structures in LaMnO_3 , *Phys. Rev. B* 56, 12154 (1997).
 [10] A. O'Hara and A. A. Demkov, Nature of the metal-insulator transition in NbO_2 , *Phys. Rev. B* 91, 094305 (2015).
 [11] S. Sarkar, R. Raghunathan, S. Chowdhury, R. J. Choudhary, and D. M. Phase, The mystery behind dynamic charge disproportionation in BaBiO_3 , *Nano Lett.* 21, 8433 (2021).
 [12] S. Gao, S. Zhang, C. Wang, S. Yan, X. Han, X. Ji, W. Tao, J. Liu, T. Wang, S. Yuan, G. Qu, Z. Chen, Y. Zhang, J. Huang, M. Pan, S. Peng, Y. Hu, H. Li, Y. Huang, H. Zhou, S. Meng, L. Yang, Z. Wang, Y. Yao, Z. Chen, M. Shi, H. Ding, H. Yang, K. Jiang, Y. Li, H. Lei, Y. Shi, H. Weng, and T. Qian, Discovery of a single-band Mott insulator in a van der Waals flat-band compound, *Phys. Rev. X* 13, 041049 (2023).
 [13] Y. Haraguchi, C. Michioka, M. Ishikawa, Y. Nakano, H. Yamochi, H. Ueda, and K. Yoshimura, Magnetic-nonmagnetic phase transition with interlayer charge disproportionation of Nb_3 trimers in the cluster

compound Nb₃Cl₈, *Inorg. Chem.* 56, 3483 (2017).

- [14] J. Hubbard and B. H. Flowers, Electron correlations in narrow energy bands, *Proc. R. Soc. A* 276, 238 (1963).
- [15] H. Zhang, Z. Shi, Z. Jiang, M. Yang, J. Zhang, Z. Meng, T. Hu, F. Liu, L. Cheng, Y. Xie, J. Zhuang, H. Feng, W. Hao, D. Shen, and Y. Du, Topological flat bands in 2D breathing-Kagome lattice Nb₃TeCl₇, *Adv. Mater.* 35, 2301790 (2023).
- [16] M. J. Wahila, G. Paez, C. N. Singh, A. Regoutz, S. Sallis, M. J. Zuba, J. Rana, M. B. Tellekamp, J. E. Boschker, T. Markurt, J. E. N. Swallow, L. A. H. Jones, T. D. Veal, W. Yang, T.-L. Lee, F. Rodolakis, J. T. Sadowski, D. Prendergast, W.-C. Lee, W. A. Doolittle, and L. F. J. Piper, Evidence of a second-order Peierls-driven metal-insulator transition in crystalline NbO₂, *Phys. Rev. Mater.* 3, 074602 (2019).
- [17] Z. Wang, O. I. Malyi, X. Zhao, and A. Zunger, Mass enhancement in 3d and s-p perovskites from symmetry breaking, *Phys. Rev. B* 103, 165110 (2021).
- [18] G. Gou, I. Grinberg, A. M. Rappe, and J. M. Rondinelli, Lattice normal modes and electronic properties of the correlated metal LaNiO₃, *Phys. Rev. B* 84, 144101 (2011).
- [19] L. Zhang, Y. Zhou, L. Guo, W. Zhao, A. Barnes, H.-T. Zhang, C. Eaton, Y. Zheng, M. Brahlek, H. F. Haneef, N. J. Podraza, M. H. W. Chan, V. Gopalan, K. M. Rabe, and R. E.-Herbert, Correlated metals as transparent conductors, *Nat. Mater.* 15, 2 (2016).
- [20] Y. Tomioka, T. Ito, E. Maruyama, S. Kimura, and I. Shindo, Magnetic and electronic properties of single crystals of perovskite nickelate oxide LaNiO₃ prepared by the laser diode floating zone method, *J. Phys. Soc. Jpn.* 90, 034704 (2021).
- [21] B. Li, D. Louca, S. Yano, L. G. Marshall, J. Zhou, and J. B. Goodenough, Insulating pockets in metallic LaNiO₃, *Adv. Electron. Mater.* 2, 1500261 (2016).
- [22] J. Sun, A. Ruzsinszky, and J. P. Perdew, Strongly constrained and appropriately normed semilocal density functional, *Phys. Rev. Lett.* 115, 036402 (2015).
- [23] S. Grytsiuk, M. I. Katsnelson, E. G. C. P. van Loon, and M. Rösner, Nb₃Cl₈: A prototypical layered Mott-Hubbard insulator, *npj Quantum Mater.* 9, 1 (2024).
- [24] M. Ströbele, J. Glaser, A. Lachgar, and H.-J. Meyer, Structure and electrochemical study of Nb₃Cl₈, *Z. Anorg. Allg. Chem.* 627, 2002 (2001).
- [25] A. Zunger, S.-H. Wei, L. G. Ferreira, and J. E. Bernard, Special quasirandom structures, *Phys. Rev. Lett.* 65, 353 (1990).
- [26] A. Baldereschi, Mean-value point in the Brillouin zone, *Phys. Rev. B* 7, 5212 (1973).
- [27] D. J. Chadi and M. L. Cohen, Special points in the Brillouin zone, *Phys. Rev. B* 8, 5747 (1973).
- [28] V. Popescu and A. Zunger, Extracting E versus k effective band structure from supercell calculations on alloys and impurities, *Phys. Rev. B* 85, 085201 (2012).
- [29] J. C. Slater, Magnetic effects and the Hartree-Fock equation, *Phys. Rev.* 82, 538 (1951).
- [30] G. Catalan, Progress in perovskite nickelate research, *Phase Transitions* 81, 729 (2008).
- [31] J. Varignon, M. N. Grisolia, J. Íñiguez, A. Barthélémy, and M. Bibes, Complete phase diagram of rare-earth nickelates from first-principles, *npj Quantum Mater.* 2, 1 (2017).
- [32] C. E. Moore, Atomic Energy Levels as Derived from the Analyses of Optical Spectra: The Spectra of Hydrogen, Deuterium, Tritium, Helium, Lithium, Beryllium, Boron, Carbon, Nitrogen, Oxygen, Fluorine, Neon, Sodium, Magnesium, Aluminum, Silicon, Phosphorus, Sulfur, Chlorine, Argon, Potassium, Calcium, Scandium, Titanium, and Vanadium (U.S. Department of Commerce, National Bureau of Standards, 1949).
- [33] C. E. Moore, A Multiplet Table of Astrophysical Interest (U.S. Department of Commerce, Office of Technical Services, 1959).
- [34] M. Imada, A. Fujimori, and Y. Tokura, Metal-insulator transitions, *Rev. Mod. Phys.* 70, 1039 (1998).
- [35] A. Fazzio and A. Zunger, Many-electron multiplet effects in the optical spectra of NiO, CoO and MnO, *Solid State Commun.* 52, 265 (1984).
- [36] A. Zunger, Electronic structure of 3d Transition-Atom Impurities in Semiconductors, in *Solid State Phys.*, edit. F. Seitz, D. Turnbull, and H. Ehrenreich (Acad Press NY) 39, 275-464 (1986).
- [37] J. S. Griffith, *The Theory of Transition-Metal Ions* (Cambridge University Press, 1971).
- [38] G. M. Lawrence and B. D. Savage, Radiative lifetimes of UV multiplets in boron, carbon, and nitrogen, *Phys. Rev.* 141, 67 (1966).

* Electronic address: alex.zunger@colorado.edu